Evaluating the locality of intrinsic precession damping in transition metals

Keith Gilmore[1,2] and Mark D. Stiles[1]
[1]*Center for Nanoscale Science and Technology, National Institute of Standards and Technology, Gaithersburg, Maryland 20899-6202, USA*
[2]*Maryland Nanocenter, University of Maryland, College Park, Maryland 20742-3511, USA*
(Received 10 January 2009; published 24 April 2009)

The Landau-Lifshitz-Gilbert damping parameter is typically assumed to be a local quantity, independent of magnetic configuration. To test the validity of this assumption we calculate the precession damping rate of small amplitude nonuniform mode magnons in iron, cobalt, and nickel. At scattering rates expected near and above room temperature, little change in the damping rate is found as the magnon wavelength is decreased from infinity to a length shorter than features probed in recent experiments. This result indicates that nonlocal effects due to the presence of weakly nonuniform modes, expected in real devices, should not appreciably affect the dynamic response of the element at typical operating temperatures. Conversely, at scattering rates expected in very pure samples around cryogenic temperatures, nonlocal effects result in an order of magnitude decrease in damping rates for magnons with wavelengths commensurate with domain-wall widths. While this low-temperature result is likely of little practical importance, it provides an experimentally testable prediction of the nonlocal contribution of the spin-orbit torque-correlation model of precession damping. None of these results exhibit strong dependence on the magnon propagation direction.

DOI: 10.1103/PhysRevB.79.132407 PACS number(s): 75.60.Jk, 75.30.Ds

Magnetization dynamics continues to be a technologically important, but incompletely understood topic. Historically, field-induced magnetization dynamics have been described adequately by the phenomenological Landau-Lifshitz (LL) equation[1]

$$\dot{\mathbf{m}} = -|\gamma_M|\mathbf{m}\times\mathbf{H} + \lambda\hat{\mathbf{m}}\times(\mathbf{m}\times\mathbf{H}), \tag{1}$$

or the mathematically equivalent Gilbert form.[2,3] Equation (1) accounts for the near equilibrium dynamics of systems in the absence of an electrical current. γ_M is the gyromagnetic ratio and λ is the phenomenological damping parameter, which quantifies the decay of the excited system back to equilibrium. The LL equation is a rather simple approximation to very intricate dynamic processes. The limitations of the approximations entering into the LL equation are likely to be tested by the next generation of magnetodynamic devices. While many generalizations for the LL equation are possible, we focus on investigating the importance of nonlocal contributions to damping. It is generally assumed in both analyzing experimental results and in performing micromagnetic simulations that damping is a local phenomenon. While no clear experimental evidence exists to contradict this assumption, the possibility that the damping is nonlocal—that it depends, for example, on the local gradient of the magnetization—would have particular implications for experiments that quantify spin-current polarization,[4] for storage[5] and logic[6] devices based on using this spin current to move domain walls, quantifying vortex[7] and mode[8] dynamics in patterned samples, and the behavior of nanocontact oscillators.[9,10]

While several viable mechanisms have been proposed to explain the damping process in different systems,[11–17] we restrict the scope of this Brief Report to investigating the degree to which the assumption of local damping is violated for small amplitude dynamics within pure bulk transition-metal systems where the dominant source of damping is the intrinsic spin-orbit interaction. For such systems, Kamberský's[14] spin-orbit torque-correlation model, which predicts a decay rate for the uniform precession mode of

$$\lambda_0 = \frac{\pi\hbar\gamma_M^2}{\mu_0}\sum_{nm}\int d\mathbf{k}|\Gamma^-_{nm}(\mathbf{k})|^2 W_{nm}(\mathbf{k}), \tag{2}$$

has recently been demonstrated to account for the majority of damping.[18,19] The matrix elements $|\Gamma^-_{nm}(\mathbf{k})|^2$ represent a scattering event in which a quantum of the uniform mode decays into a single quasiparticle electron-hole excitation. This annihilation of a magnon raises the angular momentum of the system, orienting the magnetization closer to equilibrium. The excited electron, which has wave vector $\mathbf{k}$ and band index m, and the hole, with wave vector $\mathbf{k}$ and band index n, carry off the energy and angular momentum of the magnon. This electron-hole pair is rapidly quenched through lattice scattering. The weighting function $W_{nm}(\mathbf{k})$ measures the rate at which the scattering event occurs. The very short lifetime of the electron-hole pair quasiparticle (on the order of fs at room temperature) introduces significant energy broadening (several hundred meV). The weighting function, which is a generalization of the delta function appearing in a simple Fermi's golden rule expression, quantifies the energy overlap of the broadened electron and hole states with each other and with the Fermi level.

Equation (2), which has been discussed extensively,[14,18–20] considers only local contributions to the damping rate. Nonlocal contributions to damping may be studied through the decay of nonuniform spin waves. Although recent efforts have approached the problem of nonlocal contributions to the dissipation of noncollinear excited states[21,22] the simple step of generalizing Kamberský's theory to nonuniform mode magnons has not yet been taken. We fill this obvious gap, obtaining a damping rate of

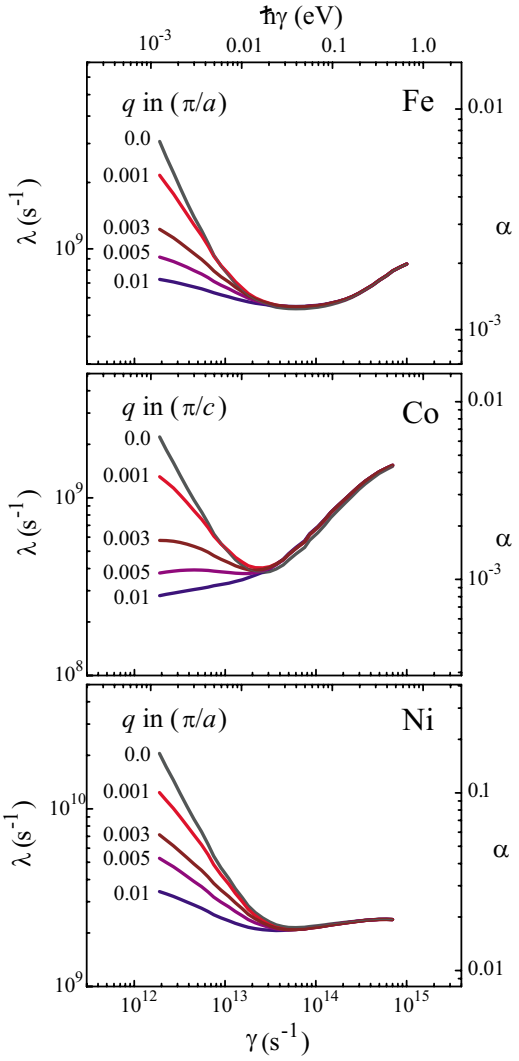

FIG. 1. (Color online) Damping rates versus scattering rate. The precession damping rates for magnons in iron, cobalt, and nickel are plotted versus electron-scattering rate for several magnon wave vectors. A dramatic reduction in damping rate is observed at the lowest scattering rates. The Landau-Lifshitz λ (Gilbert α) damping parameter is given on the left (right) axes. Electron scattering rate is given in eV on the top axis. Magnon wave-vector magnitudes are given in units of the Brillouin-zone edge and directions are as indicated in the text.

$$\lambda_{\mathbf{q}} = \frac{\pi\hbar\gamma_M^2}{\mu_0}\sum_{nm}\int d\mathbf{k}|\Gamma_{nm}^{-}(\mathbf{k},\mathbf{k}+\mathbf{q})|^2 W_{nm}(\mathbf{k},\mathbf{k}+\mathbf{q}) \quad (3)$$

for a magnon with wave vector $\mathbf{q}$. We test the importance of nonlocal effects by quantifying this expression for varying degrees of magnetic noncollinearity (magnon wave-vector magnitude). The numerical evaluation of Eq. (3) for the damping rate of finite wavelength magnons in transition-metal systems, presented in Fig. 1, and the ensuing physical discussion form the primary contribution of this Brief Report. We find that the damping rate expected in very pure samples at low temperature is rapidly reduced as the magnon wave vector $|\mathbf{q}|$ grows, but the damping rate anticipated outside of this ideal limit is barely affected. We provide a simple band-structure argument to explain these observations. The results are relevant to systems for which the noncollinear excitation may be expanded in long-wavelength spin waves, provided the amplitude of these waves is small enough to neglect magnon-magnon scattering.

Calculations for the single-mode damping constant [Eq. (3)] as a function of electron-scattering rate are presented in Fig. 1 for iron, cobalt, and nickel. The Gilbert damping parameter $\alpha=\lambda/\gamma_M$ is also given. Damping rates are given for magnons with wave vectors along the bulk equilibrium directions, which are ⟨100⟩ for Fe, ⟨0001⟩ for Co, and ⟨111⟩ for Ni. Qualitatively and quantitatively similar results were obtained for other magnon wave-vector directions for each metal. The magnons reported in Fig. 1 constitute small deviations of the magnetization transverse to the equilibrium direction with wave-vector magnitudes between zero and 1% of the Brillouin-zone edge. This wave-vector range corresponds to magnon half-wavelengths between infinity and 100 lattice spacings, which is 28.7 nm for Fe, 40.7 nm for Co, and 35.2 nm for Ni. This range includes the wavelengths reported by Vlaminck and Bailleul in their recent measurement of spin polarization.[4]

Results for the three metals are qualitatively similar. The most striking trend is a dramatic order of magnitude decrease in the damping rate at the lowest scattering rate tested as the wave-vector magnitude increases from zero to 1% of the Brillouin-zone edge. This observation holds in each metal for every magnon propagation direction investigated. For the higher scattering rates expected in devices at room temperature there is almost no change in the damping rate as the magnon wave vector increases from zero to 1% of the Brillouin-zone edge in any of the directions investigated for any of the metals.

To understand the different dependences of the damping rate on the magnon wave vector at low versus high scattering rates we first note that the damping rate [Eqs. (2) and (3)] is a convolution of two factors: the torque matrix elements and the weighting function. The matrix elements do not change significantly as the magnon wave vector increases, however, the weighting function can change substantially. The weighting function

$$W_{nm}(\mathbf{k},\mathbf{k}+\mathbf{q}) \approx A_{n,\mathbf{k}}(\epsilon_F)A_{m,\mathbf{k}+\mathbf{q}}(\epsilon_F) \quad (4)$$

contains a product of the initial and final-state electron spectral functions

$$A_{n,\mathbf{k}}(\epsilon) = \frac{1}{\pi}\frac{\hbar\gamma}{(\epsilon-\epsilon_{n,\mathbf{k}})^2+(\hbar\gamma)^2}, \quad (5)$$

which are Lorentzians in energy space. The spectral function for state $|n,\mathbf{k}\rangle$, which has nominal band energy $\epsilon_{n,\mathbf{k}}$, is evaluated within a very narrow range of the Fermi level ϵ_F. The width of the spectral function $\hbar\gamma$ is given by the electron-scattering rate $\gamma=1/2\tau$, where τ is the orbital lifetime. (The lifetimes of all orbital states are taken to be equal for these calculations and no specific scattering mechanism is implied.) The weighting function restricts the electron-hole pair generated during the magnon decay to states close in energy

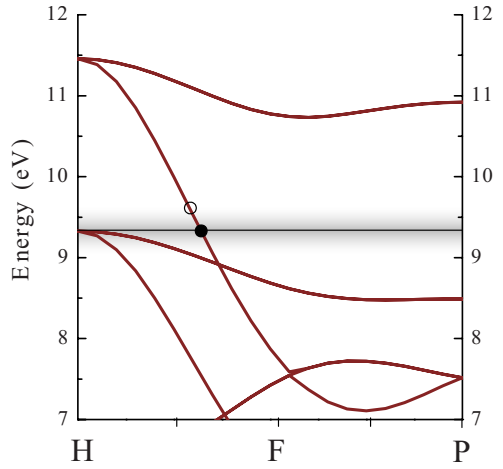

FIG. 2. (Color online) Partial band structure of bcc iron. The horizontal black line indicates the Fermi level and the shaded region represents the degree of spectral broadening. The solid dot is a hypothetical initial electron state while the open circle is a potential final scattering state. (Initial and final state wave-vector separations are exaggerated for clarity of illustration.) The intraband magnon decay rate diminishes as the energy separation of the states exceeds the spectral broadening.

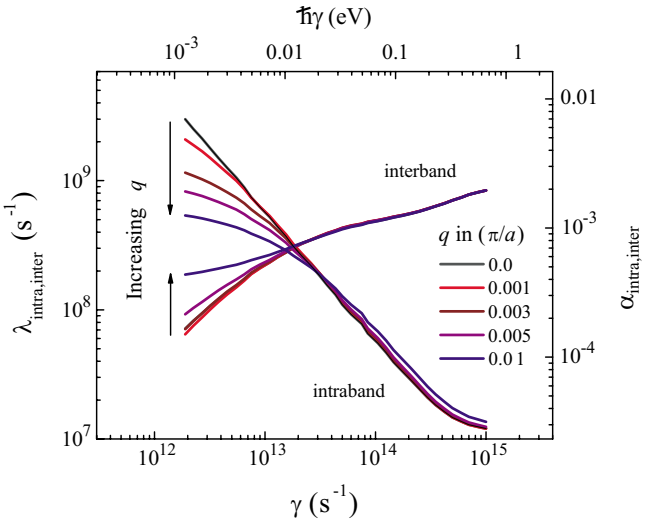

FIG. 3. (Color online) Intraband and interband damping contributions in iron. The intraband and interband contributions to the damping rate of magnons in the ⟨100⟩ direction in iron are plotted versus scattering rate for several magnitudes of magnon wave vector. Magnitudes are given in units of the Brillouin-zone edge.

to each other and near the Fermi level. For high scattering rates, the electron spectral functions are significantly broadened and the weighting function incorporates states within an appreciable range (several hundred meV) of the Fermi level. For low scattering rates, the spectral functions are quite narrow (only a few meV) and both the electron and hole state must be very close to the Fermi level.

The second consideration useful for understanding the results of Fig. 1 is that the sum in Eqs. (2) and (3) can be divided into intraband ($n=m$) and interband ($n \neq m$) terms. For the uniform mode, these two contributions correspond to different physical processes with the intraband contribution dominating at low scattering rates and the interband terms dominating at high scattering rates.[14,18–20]

For intraband scattering, the electron and hole occupy the same band and must have essentially the same energy (within $\hbar\gamma$). The energy difference between the electron and hole states may be approximated as $\epsilon_{n,\mathbf{k}+\mathbf{q}} - \epsilon_{n,\mathbf{k}} \approx \mathbf{q} \cdot \partial\epsilon_{n,\mathbf{k}}/\partial\mathbf{k}$. The generation of intraband electron-hole pairs responsible for intraband damping gets suppressed as $\mathbf{q} \cdot \partial\epsilon_{n,\mathbf{k}}/\partial\mathbf{k}$ becomes large compared to $\hbar\gamma$. Unless the bands are very flat at the Fermi level there will be few locations on the Fermi surface that maintain the condition $\mathbf{q} \cdot \partial\epsilon_{n,\mathbf{k}}/\partial\mathbf{k} < \hbar\gamma$ for low scattering rates as the magnon wave vector grows (see Fig. 2). Indeed, at low scattering rates when $\hbar\gamma$ is only a few meV, Fig. 3 shows that the intraband contribution to damping decreases markedly with only modest increase in the magnon wave vector. Since the intraband contribution dominates the interband term in this limit the total damping rate also decreases sharply as the magnon wave vector is increased for low scattering rates. For higher scattering rates, the electron spectral functions are sufficiently broadened that the overlap of intraband states does not decrease appreciably as the states are separated by finite wave vector ($\mathbf{q} \cdot \partial\epsilon_{n,\mathbf{k}}/\partial\mathbf{k} < \hbar\gamma$ generally holds over the Fermi surface). Therefore, the intraband contribution is largely independent of magnon wave vector at high scattering rates.

The interband contribution to damping involves scattering between states in different bands, separated by the magnon wave vector $\mathbf{q}$. Isolating the interband damping contribution reveals that these contributions are insensitive to the magnon wave vector at higher scattering rates where they form the dominant contribution to damping (see Fig. 3). To understand these observations we again compare the spectral broadening $\hbar\gamma$ to the quasiparticle energy difference $\Delta_{n,\mathbf{k}}^{m,\mathbf{k}+\mathbf{q}} = \epsilon_{m,\mathbf{k}+\mathbf{q}} - \epsilon_{n,\mathbf{k}}$. The quasiparticle energy difference may be approximated as $\Delta_{n,\mathbf{k}}^{m,\mathbf{k}} + \mathbf{q} \cdot \partial\Delta_{n,\mathbf{k}}^{m,\mathbf{k}}/\partial\mathbf{k}$. The interband energy spacings are effectively modulated by the product of the magnon wave vector and the slopes of the bands. At high scattering rates, when the spectral broadening exceeds the vertical band spacings, this energy modulation is unimportant and the damping rate is independent of the magnon wave vector. At low scattering rates, when the spectral broadening is less than many of the band spacings, this modulation can alter the interband energy spacings enough to allow or forbid generation of these electron-hole pairs. For Fe, Co, and Ni, this produces a modest increase in the interband damping rate at low scattering rates as the magnon wave vector increases. However, this effect is unimportant to the total damping rate, which remains dominated by the intraband terms at low scattering rates.

Lastly, we describe the numerical methods employed in this study. Converged ground-state electron densities were first obtained via the linear-augmented-plane-wave method. The Perdew-Wang functional for exchange-correlation within the local spin-density approximation was implemented. Many details of the ground-state density convergence process are given in Ref. 23. Densities were then expanded into Kohn-Sham orbitals using a scalar-relativistic spin-orbit interaction with the magnetization aligned along the experimentally determined magnetocrystalline anisotropy

easy axis. The Kohn-Sham energies were artificially broadened through the *ad-hoc* introduction of an electron lifetime. Matrix elements of the torque operator $\Gamma^- = [\sigma^-, \mathcal{H}_{so}]$ were evaluated similarly to the spin-orbit matrix elements.[24] (σ^- is the spin lowering operator and $\mathcal{H}_{so}$ is the spin-orbit Hamiltonian.) The product of the matrix elements and the weighting function were integrated over k space using the special-point method with a fictitious smearing of the Fermi surface for numerical stability. Convergence was obtained by sampling the full Brillouin zone with 160^3 k points for Fe and Ni, and $160^2 \times 91$ points for Co.

In summary, we have investigated the importance of nonlocal damping effects by calculating the intrinsic spin-orbit contribution to precession damping in bulk transition-metal ferromagnets for small amplitude spin waves with finite wavelengths. Results of the calculations do not contradict the common-practice assumption that damping is a local phenomenon. For transition metals, at scattering rates corresponding to room temperature, we find that the single-mode damping rate is essentially independent of magnon wave vector for wave vectors between zero and 1% of the Brillouin-zone edge. It is not until low temperatures in the most pure samples that nonlocal effects become significant. At these scattering rates, damping rates decrease by as much as an order of magnitude as the magnon wave vector is increased. The insensitivity of damping rate to magnon wave vector at high scattering rates versus the strong sensitivity at low scattering rates can be explained in terms of band-structure effects. Due to electron spectral broadening at high scattering rates the energy conservation constraint during magnon decay is effectively relaxed, making the damping rate independent of magnon wave vector. The minimal spectral broadening at low scattering rates—seen only in very pure and cold samples—greatly restricts the possible intraband scattering processes, lowering the damping rate. The prediction of reduced damping at low scattering rates and nonzero magnon wave vectors is of little practical importance, but could provide an accessible test of the torque-correlation model. Specifically, this might be testable in ferromagnetic semiconductors such as (Ga,Mn)As for which many spin-wave resonances have been experimentally observed at low temperatures.[25]

This work has been supported in part through NIST-CNST/UMD-Nanocenter cooperative agreement.

[1] L. Landau and E. Lifshitz, Phys. Z. Sowjetunion **8**, 153 (1935).
[2] T. L. Gilbert, Armour Research Foundation Report No. A059, 1956.
[3] T. L. Gilbert, IEEE Trans. Magn. **40**, 3443 (2004).
[4] V. Vlaminck and M. Bailleul, Science **322**, 410 (2008).
[5] S. S. P. Parkin, M. Hayashi, and L. Thomas, Science **320**, 190 (2008).
[6] M. Hayashi, L. Thomas, R. Moriya, C. Rettner, and S. S. P. Parkin, Science **320**, 209 (2008).
[7] B. E. Argyle, E. Terrenzio, and J. C. Slonczewski, Phys. Rev. Lett. **53**, 190 (1984).
[8] R. D. McMichael, C. A. Ross, and V. P. Chuang, J. Appl. Phys. **103**, 07C505 (2008).
[9] S. Kaka, M. R. Pufall, W. H. Rippard, T. J. Silva, S. E. Russek, and J. A. Katine, Nature (London) **437**, 389 (2005).
[10] F. B. Mancoff, N. D. Rizzo, B. N. Engel, and S. Tehrani, Nature (London) **437**, 393 (2005).
[11] B. Heinrich, D. Fraitová, and V. Kamberský, Phys. Status Solidi **23**, 501 (1967).
[12] V. Kamberský, Can. J. Phys. **48**, 2906 (1970).
[13] V. Korenman and R. E. Prange, Phys. Rev. B **6**, 2769 (1972).
[14] V. Kamberský, Czech. J. Phys., Sect. B **26**, 1366 (1976).
[15] J. Sinova, T. Jungwirth, X. Liu, Y. Sasaki, J. K. Furdyna, W. A. Atkinson, and A. H. MacDonald, Phys. Rev. B **69**, 085209 (2004).
[16] Y. Tserkovnyak, A. Brataas, and G. E. W. Bauer, Phys. Rev. Lett. **88**, 117601 (2002).
[17] M. Zwierzycki, Y. Tserkovnyak, P. J. Kelly, A. Brataas, and G. E. W. Bauer, Phys. Rev. B **71**, 064420 (2005).
[18] K. Gilmore, Y. U. Idzerda, and M. D. Stiles, Phys. Rev. Lett. **99**, 027204 (2007).
[19] V. Kamberský, Phys. Rev. B **76**, 134416 (2007).
[20] K. Gilmore, Y. U. Idzerda, and M. D. Stiles, J. Appl. Phys. **103**, 07D303 (2008).
[21] M. Fähnle and D. Steiauf, Phys. Rev. B **73**, 184427 (2006).
[22] J. Foros, A. Brataas, Y. Tserkovnyak, and G. E. W. Bauer, Phys. Rev. B **78**, 140402(R) (2008).
[23] L. F. Mattheiss and D. R. Hamann, Phys. Rev. B **33**, 823 (1986).
[24] M. D. Stiles, S. V. Halilov, R. A. Hyman, and A. Zangwill, Phys. Rev. B **64**, 104430 (2001).
[25] S. T. B. Goennenwein, T. Graf, T. Wassner, M. S. Brandt, M. Stutzmann, A. Koeder, S. Frank, W. Schoch, and A. Waag, J. Supercond. **16**, 75 (2003).